RESEARCH ARTICLE

Macromolecular Chemistry and Physics
www.mcp-journal.de

Functionalized Electron-Rich Pyridines as Initiators for the Epoxy Homopolymerization

*David Edinger, Susanne M. Fischer, and Christian Slugovc**

A simple and modular dialkylation of two electron-rich pyridine derivatives, namely 4-aminopyridine or 1,2,3,4-tetrahydropyrido[3,4-b]pyrazine, is achieved by aza-Michael reactions with electron-poor olefins (ethyl acrylate and acrylonitrile). Reducing the ester groups in the ethyl acrylate-derived compounds yielded the corresponding hydroxyl-containing derivatives. Subsequently, homopolymerization of phenyl glycidyl ether as well as an epoxy-alcohol polyaddition are catalyzed using the introduced compounds. As a reference catalyst, 4-dimethylaminopyridine is used. It is found that in all cases an irreversible termination of the polymerization at temperatures above 100 °C occurred. The decomposition is particularly rapid in the case of pyridine derivatives containing hydroxyl groups. In contrast, at a constant temperature of 100 °C, the latter compounds gave the fastest phenyl glycidyl ether homopolymerization and high conversions are found for all electron-rich pyridine derivatives. However, testing the catalysts at high alcohol concentrations at temperatures higher than 100 °C resulted in similarly moderate conversions in all cases.

1. Introduction

4-(Dimethylamino)pyridine (DMAP) and related Lewis bases are widely used reagents for acylation, alkylation, condensation, and transesterification reactions.[1,2] In polymer chemistry, DMAP is used as a catalyst/initiator for living ring-opening polymerization of lactide,[3] in the conversion of isocyanates with alcohols[4] or as the initiator for aza-[5] and oxa-Michael polymerizations.[6–9] Further, DMAP is used in the homopolymerization of epoxy monomers[10,11] and in the combined polymerization of epoxy monomers and esters[11–15] as well as in the carbon dioxide addition to epoxides[16,17] and in the ring-opening polymerization of cyclic carbonates.[18] In these cases, the use of DMAP often suffers from its poor solubility in the formulations. Since the use of solvents is usually undesirable, there is a strong interest in developing an easy and modular synthetic route to prepare DMAP analogues with tunable solubility. Another motivation is to provide a convenient method for incorporating additional functional groups, such as those used for polymerization or immobilization of DMAP derivatives,[19,20] or for tuning the activity of the catalysts.

Herein we disclose a synthetic methodology based on the aza-Michael reaction[21] of 4-aminopyridine or 1,2,3,4-tetrahydropyrido[3,4-b]pyrazine with electron-poor olefins, namely acrylonitrile and ethyl acrylate, and test the performance of the obtained derivatives and their follow-up products (**Scheme 1**) in epoxy homopolymerization as well as in the epoxy-alcohol reaction. In this context, we are particularly interested in discovering the activity of electron-rich pyridines with additional hydroxyl groups, which, as will be shown, are easily accessible via the synthetic route discussed.

DMAP is usually prepared by reacting dimethylamine with 1-(4-pyridyl)pyridinium chloride, which is accessible from pyridine and chlorine.[22] In contrast, here we start from 4-aminopyridine, accessible either via ammonolysis of 1-pyridylpyridinium dichloride or via a Hofmann rearrangement of the corresponding pyridinecarboxamide[23] and perform an aza-Michael reaction for the alkylation. This synthetic approach should also be readily applicable to the derivatization of other more complex electron-rich aminopyridines, as exemplified here by the synthesis of alkyl-substituted 3,4-diaminopyridines.[24]

2. Results and Discussion

Firstly, the use of acrylonitrile as electron-poor olefin was investigated in the synthesis of the doubly cyanoethylated aminopyridine derivative (1a). Compound 1a is readily obtained by heating 4-aminopyridine in acrylonitrile at 80 °C for 24 h in 68% yield (**Scheme 2**). The synthesis of 1a has been described in the literature using the same synthetic approach, but higher yields have been reported.[25,26] Compound 1a has been used as an intermediate in the preparation of polymeric acylation catalysts.[27] A single crystal X-ray structure of 1a is available.[25]

D. Edinger, S. M. Fischer, C. Slugovc
Institute for Chemistry and Technology of Materials
Technische Universität Graz
Stremayrgasse 9, Graz 8010, Austria
E-mail: slugovc@tugraz.at
D. Edinger, S. M. Fischer, C. Slugovc
Christian Doppler Laboratory for Organocatalysis in Polymerization
Stremayrgasse 9, Graz 8010, Austria

The ORCID identification number(s) for the author(s) of this article can be found under https://doi.org/10.1002/macp.202300299

DOI: 10.1002/macp.202300299

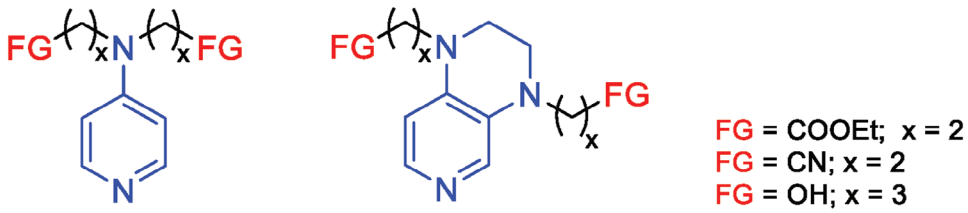

Scheme 1. Electron- rich pyridine derivatives under investigation.

In contrast, 3,3′-(2,3-dihydropyrido[3,4-b]pyrazine-1,4-diyl)bis[propanenitrile] (1b) is a previously unknown compound, which was prepared by heating a dispersion of 1,2,3,4-tetrahydropyrido[3,4-b]pyrazine in acrylonitrile for 24 h at 80 °C. Upon removal of volatiles, an oily brown residue remained from which 1b was isolated by column chromatography in 61% yield.

Changing to ethyl acrylate as the Michael-acceptor, N-(3-ethoxy-3-oxopropyl)-N-4-pyridinyl-β-alanine ethyl ester (2a) was obtained in 43% yield by reacting 4-aminopyridine and ethyl acrylate at 80 °C for 24 h. Compound 2a has been previously disclosed in a patent[28] and the corresponding dimethyl ester derivative is also known.[27,29,30] The moderate yield is due to the need to separate ethyl acrylate oligomers by column chromatography. One of these by-products was obtained in pure form and was identified as 2a' (**Figure 1**). In contrast to 2a, the ^{1}H-NMR spectrum of 2a' shows the presence of three ethyl ester groups (CH_2 at 4.2–4.1 ppm and CH_3 at 1.27–1.16 ppm) per pyridine moiety, rather than two as in 2a. The 2-substituted pentanedioate substructure gives rise to a multiplet with the relative intensity of one proton at 2.83 ppm and two multiplets at 2.33 and 1.89 ppm. 2a' is probably formed by a carba-Michael reaction of 2a with surplus ethyl acrylate.[31]

It is interesting to note that no related byproducts were observed when imidazoles were used as Michael donors under similar reaction conditions.[32] The product of the double Michael addition of ethyl acrylate to 1,2,3,4-tetrahydropyrido[3,4-b]pyrazine (2b) is obtained in a similar way. Again, column chromatography was used to purify the target compound, which was obtained in 40% yield. The two diesters 2a and 2b were then reduced with lithium aluminum hydride to give the corresponding dialcohols 3a and 3b in 60% and 50% yield respectively (**Scheme 3**).

In the next step, the synthesized electron-rich pyridine derivatives were tested as catalysts/initiators in the homopolymerization of phenyl glycidyl ether (PGE). The reaction was monitored using dynamic differential scanning calorimetry (DSC)[10] accompanied by online monitoring of sample weights in a simultaneous thermal analysis (STA) instrument. The reaction has previously been studied under solvent-free conditions with a DMAP loading of 2 or 8 mol%.[10] However, the solubility of DMAP and the compounds prepared here in PGE at room temperature is only moderate and from our experience, loadings above 5 mol% are not fully soluble in the monomer within minutes at room temperature. The solubility of compounds 1b and 2b in PGE is particularly poor and therefore these two compounds were not evaluated in the following. Results are shown in **Figure 2**. The benchmark experiment with DMAP as the initiator shows an onset of the polymerization at about 80 °C, a maximum of the heat flow at 129 ± 1 °C, and heat of polymerization of about 96 ± 3 kJ mol^{-1}. At the same time, a mass loss of 16 ± 2% is observed at a temperature of 210 °C, indicating that no complete polymerization of PGE could be obtained under these curing conditions. The cyanoethylated compound 1a shows a much later onset of the polymerization (as indicated by the exothermic heat flow in the thermogram) at about 125 °C. Shortly before this, at about 118 °C, an endothermic event is observed, which could be due to the dissolution of crystals of 1a (indeed, the solubility of 1a in PGE is the lowest of all the molecules studied). The heat flux peaks at 141 ± 1 °C and probably a lower heat of polymerization

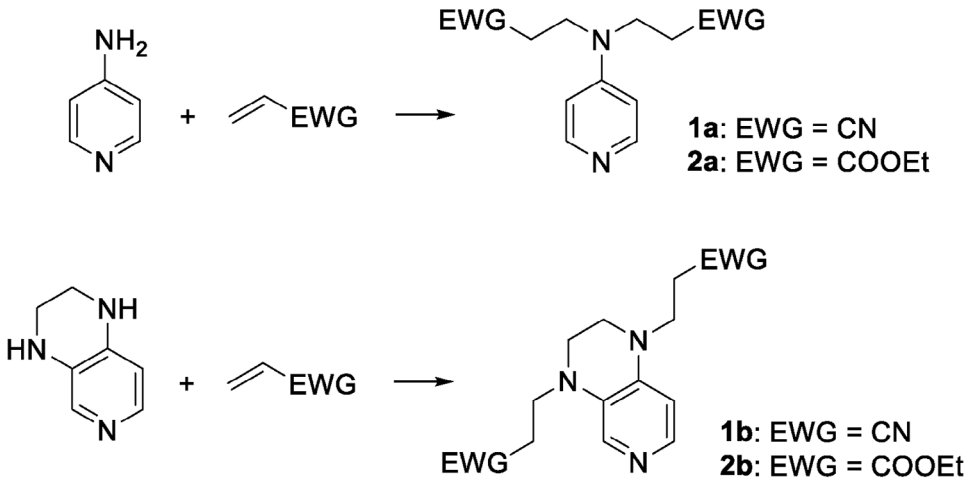

Scheme 2. Preparation of compounds 1a- 2b.

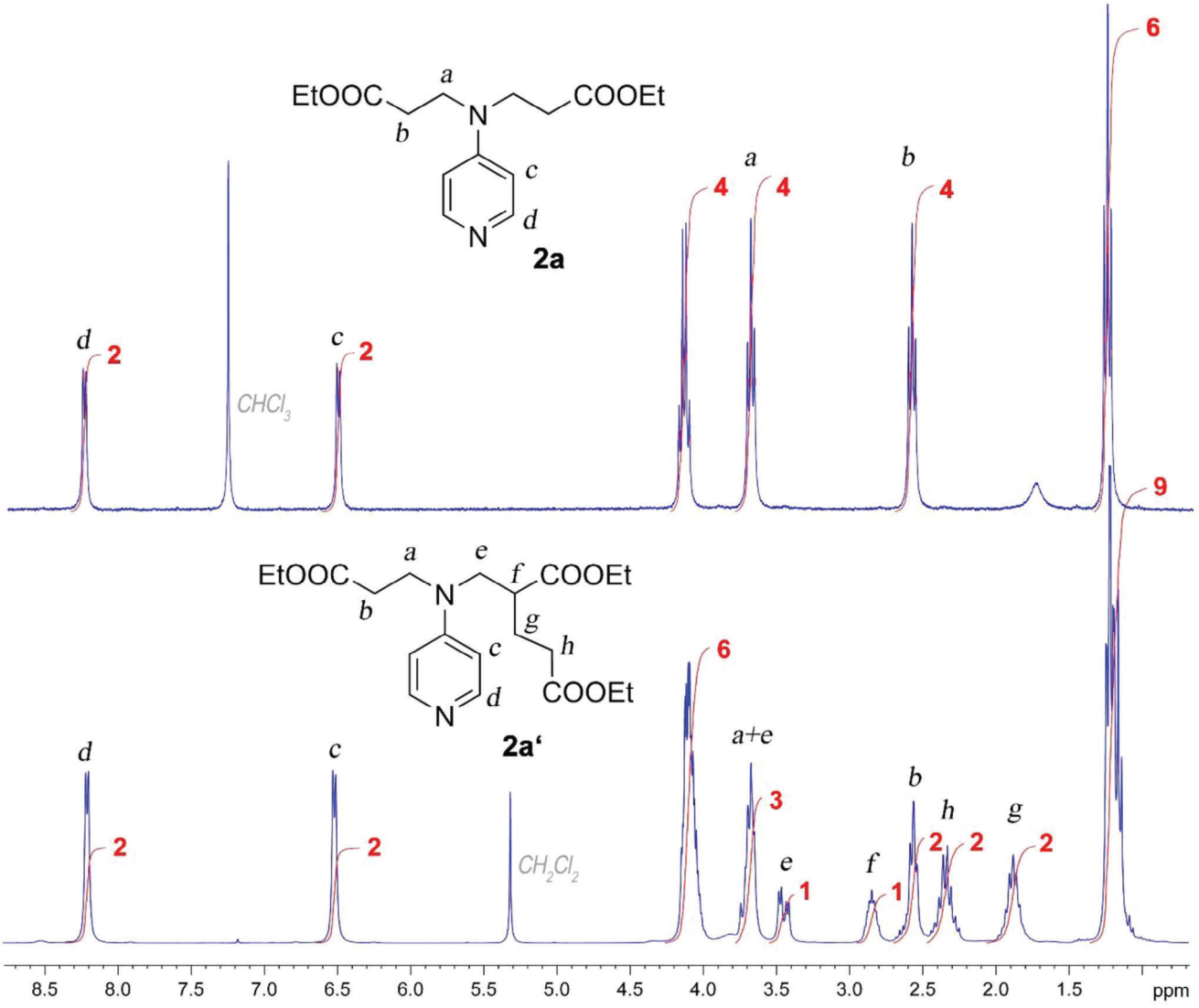

Figure 1. ^{1}H-NMR spectra of 2a and 2a' recorded in $CDCl_3$ at 300 MHz; the red numbers correspond to the integrals of the peaks and letters are used for the peak assignments.

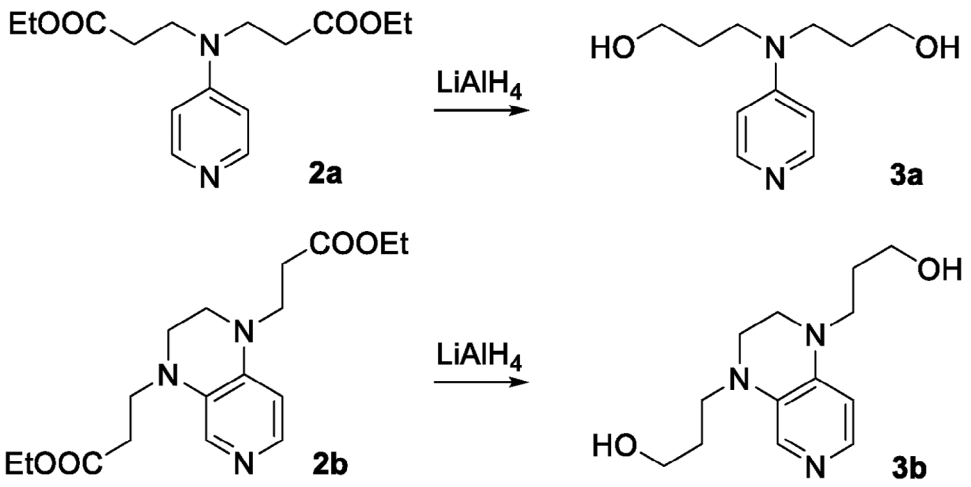

Scheme 3. Preparation of compounds 3a and 3b.

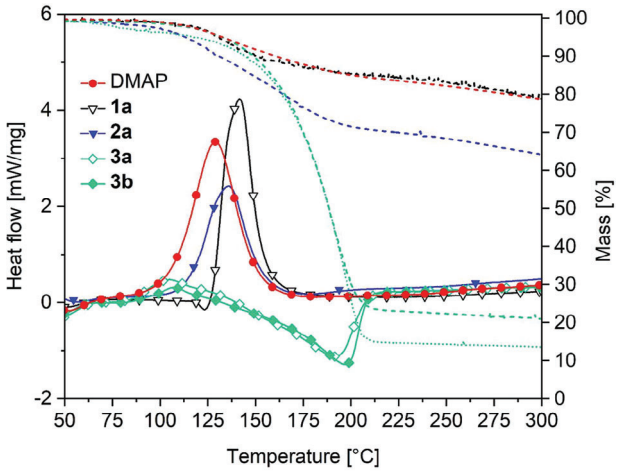

Figure 2. Dynamic STA measurements of the homopolymerization of PGE initiated with 1a, 2a, 3a, 3b, and DMAP (5 mol% in respect to PGE; Heat rate = 10 K min^{-1}) showing the heat flow of DSC experiments (thick lines with symbols, exothermal reactions show a positive heat flow) and the masses of the samples in dependence of the temperature (dashed lines with the same color code).

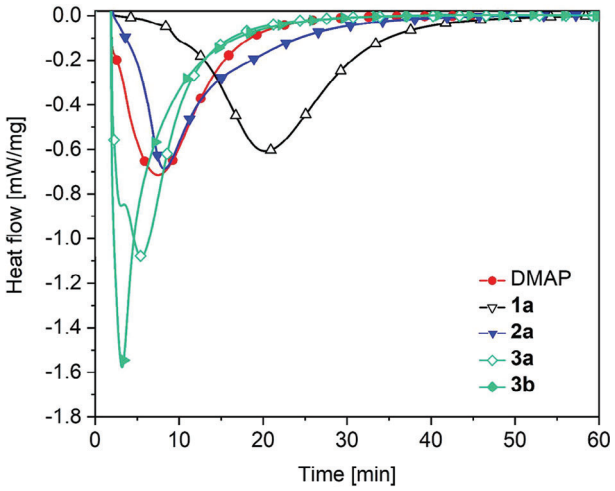

Figure 3. Isothermal DSC measurements of the homopolymerization of PGE initiated with 1a, 2a, 3a, 3b, and DMAP (5 mol% in respect to PGE; Reaction temperature: 100 °C) showing the heat flow (exothermal events show a negative heat flow).

was evolved (>80 kJ mol^{-1}, the simultaneous occurrence of an endothermic heat flux prevents a more accurate quantification) than in the case of DMAP. However, the mass loss observed in this experiment is very similar (16 ± 2% at 210 °C) to that found in the DMAP experiment, suggesting similar PGE conversions in both cases. In the case of the diethyl ester derivative 2a, the onset of polymerization is found at a temperature about 20 °C lower than in the case of 1a, but still considerably higher than in the case of DMAP. The heat flux has its maximum at about 136 ± 1 °C and the heat of reaction is much lower at 70 ± 3 kJ mol^{-1}, which is accompanied by a much higher mass loss of about 30 ± 1% at 210 °C. It is interesting to note that the mass loss already starts at about 100 °C, that is, at a much lower temperature than in the case of DMAP or 1a. Based on the literature,[11–15] transesterification can be assumed to occur simultaneously with the anionic polymerization of PGE, which slows down the propagation reaction. A similar situation is conceivable for 1a, where the attack of the alkoxide on the electrophilic carbon atom of the nitrile may slow the propagation. Finally, diol derivatives 3a and 3b show an early onset of the polymerization (similar to that of DMAP), but almost no heat of polymerization (in the range of 7–14 kJ mol^{-1}) could be detected. Instead, almost 80% mass loss was observed at 215 °C in the case of 3a and even 85% in the case of 3b, indicating the occurrence of deactivation reactions at elevated temperatures (becoming important above 110 °C) specific to these two pyridine derivatives. Deactivation of DMAP during homopolymerization has been described in the literature. It is believed, that the propagating ion pair (or zwitterion) is irreversibly consumed by the attack of an alkoxide on the π-system of a pyridinium cation (vide infra).[10,11] Since in the case of 3a and 3b the alcohol groups are in close proximity to the pyridinium moiety, it is easily conceivable that such degradation is more favored than in the case of DMAP or derivatives 1a and 2a.

To further qualify the different initiators, isothermal curing of PGE in the presence of 5 mol% initiator at a fixed temperature of 100 °C (temperature chosen in the range where 3a and 3b still showed heat release in the previous experiments) was studied by DSC (**Figure 3**). Under these conditions, 3a and especially the slightly better PGE soluble 3b clearly outperformed DMAP and the other newly introduced derivatives 1a and 1b. Initiator 3b shows a very fast PGE polymerization as indicated by the maximum heat flux at only 3 ± ½ min and heat of polymerization of 84 ± 2 kJ mol^{-1}. 3a behaves similarly (observed heat of reaction 83.5 ± 2 kJ mol^{-1}), but the shape of the thermogram differs from the expected shape due to the presence of an additional endothermic event (probably dissolution of 3a in PGE).

The heat of reaction reported for the polymerizations initiated with 3a and 3b can be considered as the lower limits and are most probably higher (because considerable heat of polymerization could have developed during the first 2 min of the measurement, which is needed to reach the constant temperature of 100 °C). Investigating the reaction mixture after 2 h at 100°C revealed polymerization of PGE (M_n = 800, Đ = 1.6, Figure S1, Supporting Information-with less than 3% residual PGE Figure S2, Supporting Information). DMAP is giving a slower reaction as can be seen from the time taken to reach the maximum heat flux of about 6 min, and the heat of polymerization is 68 ± 2 kJ mol^{-1} lower than for 3a or 3b. Apparently, the alcohol groups attached to the electron-rich pyridine derivatives are advantageous for fast conversion of PGE, which is in agreement with previous findings in the literature.[11] The reaction initiated by 2a starts slightly slower than in the DMAP case and takes significantly longer to complete the polymerization. A heat of polymerization of 72 ± 2 kJ mol^{-1} was measured in this case. Finally, 1a is by far the slowest initiator, showing a maximum heat flow at about 22 min. However, the highest PGE conversion was observed, as the highest heat of polymerization (90 ± 2 kJ mol^{-1}) was determined in this case. The nitrile groups appear to have some mitigating effect on the irreversible termination reaction.

To test the derivatives in an alcohol-rich environment, the curing of glycerol diglycidyl ether (gly-DGE, glycerol with an

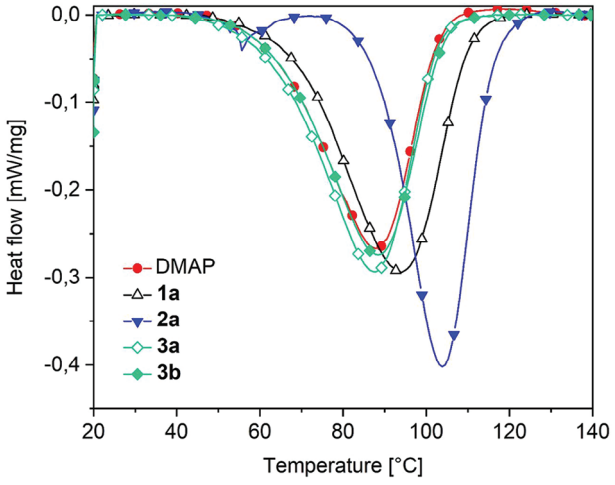

Figure 4. Dynamic DSC measurements of the epoxy alcohol reaction of Gly-DGE and (E)-but-2-ene-1,4-diol (molar ratio = 1:1) initiated with 1a, 2a, 3a, 3b, and DMAP (5 mol% in respect to PGE; heat rate = 2 K min^{-1}) showing the heat flow of DSC experiments (exothermal reactions show a negative heat flow).

average of 1.5 glycidyl ether groups) with (Z)-but-2-ene-1,4-diol (molar ratio 1:1), as an exemplary epoxy alcohol formulation, was performed[33] (**Figure 4**).

Under these conditions, 3a and 3b perform similarly to DMAP in terms of the onset of the polymerization (46 ± 2 °C) and the maximum of the thermograms at (88 ± 1 °C). However, the detected heat of polymerization is slightly lower for DMAP (42 ± 2 kJ mol^{-1}) compared to 3a and 3b (45 ± 2 kJ mol^{-1}). 1a shows a slightly delayed polymerization (maximum at 97 ± 1 °C) with a slightly higher heat of reaction (49 ± 2 kJ mol^{-1}) compared to the previous cases. The diester derivative 2a shows a different polymerization behavior. While the onset of the exothermic heat flow is at a similar temperature as in the other cases, only a small amount of heat (< 3 kJ mol^{-1}) is released. Starting at about 74 ± 1 °C, a second much stronger exothermic heat flux (46 ± 2 kJ mol^{-1}) is observed, peaking at about 104 ± 1 °C. The reason for this particular behavior is not clear at this stage. Comparing the shape and integral of the heat-flows of these experiments shows that the newly introduced alcohol-containing compounds 3a and 3b do not perform better than the parent DMAP in the epoxy-alcohol reaction. Considering that the theoretical heat of epoxy (homo)polymerization as well as epoxy-alcohol polymerization is about 100 kJ mol^{-1}[33,34] it can be concluded that under the experimental conditions, all investigated derivatives are deactivated before the monomers are completely consumed and only epoxy conversions of about 50% were obtained. NMR investigations of the samples after the DSC run revealed conversions of 58 ± 5% (Figure S3, Supporting Information). The results show that in the presence of excess hydroxyl groups, all reactions are irreversibly terminated before the epoxy groups are consumed.

The results obtained allow outlining a better mechanistic understanding, in particular with respect to the role of the alkoxide in DMAP-initiated epoxy polymerizations. First, DMAP reacts with an epoxy monomer in an equilibrium reaction to form the zwitterionic species I (**Scheme 4**). In the absence of alcohol, the alkoxide group in I can attack another PGE leading to propagation as illustrated by the homologous zwitterion II. In the presence of alcohols, the zwitterion I is removed from the equilibrium by a proton transfer reaction to form the ion-pair III, consisting of a pyridinium cation and an alkoxide, which then attacks another PGE molecule (IV) starting the propagation. The ion-pair pathway then allows a faster conversion of PGE, presumably simply because the concentration of active species (the alkoxide) is higher in this case.[35] The superior activity of 3a and 3b under isothermal curing conditions (at 100 °C) can therefore be rationalized by a switch from the zwitterionic to the ion pair pathway (Scheme 4, note that in the case of 3a or 3b and the ion pair pathway, the propagating species can be a zwitterion). Propagation can be terminated in a number of ways that cancel out the charges. Most of the termination reactions discussed involve hydrogen abstraction (β-elimination) and nucleophilic substitution by alkoxides (not shown in Scheme 4).[35] These two processes release the Lewis base and allow the polymerization to be restarted as long as unreacted epoxy groups are present.[11,36]

However, as seen previously[10] and in this study, DMAP derivatives undergo additional termination reactions leading to deactivation of the Lewis base in the presence of alkoxide. It has been suggested that the formation of species represented by V (intra- or intermolecular attack of the alkoxide on the pyridinium cation may occur) is responsible for the irreversible termination of the epoxy homopolymerization.[10] Such a deactivation reaction becomes more important at temperatures above 100 °C and more alkoxide species are present. In the case of hydroxyl group bearing 3a and 3b, the decomposition in an epoxy-homopolymerization is rapid above 100 °C resulting in the termination of PGE consumption. **Figure 5** outlines a hypothetical scenario for 3a that attempts to explain the decomposition reaction based on the reactivity of pyridinum ions.[37] Upon initiation, the zwitterion Ia is formed,[38] which is in equilibrium with the zwitterion IIIa, which in turn may undergo an intramolecular cyclization reaction to give the neutral VIa. Previously postulated species of type V,[10] such as Va sketched here, should be less important for the irreversible termination of the reaction, according to the findings made here. This is supported by the fact that the deactivation of the polymerization of PGE is fastest at elevated temperatures with the initiators 3a and 3b bearing alcohol groups. For these two compounds, intramolecular attack in the α-position to the nitrogen atom in the pyridinium ring is unlikely for steric reasons. DFT calculations of the relative energies of the structures Ia–VIa in comparison to the starting materials show no significant thermodynamic preference for one of the investigated structures.

Furthermore, due to the relatively high energy differences observed, Va or VIb should rather be considered intermediates than final products of the attack of the alkoxide at the pyridinium moiety. We expect these intermediates to be starting points for yet unknown follow-up reactions leading to thermodynamically more favored products and thus, the deactivation of the anionic polymerization reaction. The decomposition reaction starting from Ia to give Va should be equally feasible for all studied DMAP derivatives and the formation of the five-membered ring structure present in Va should be preferred over the formation of higher macrocycles or an intermolecular reaction. Accordingly, we postulate that the alkoxide attack on the other electrophilic carbon leading type VIa molecules is at least another reasonable

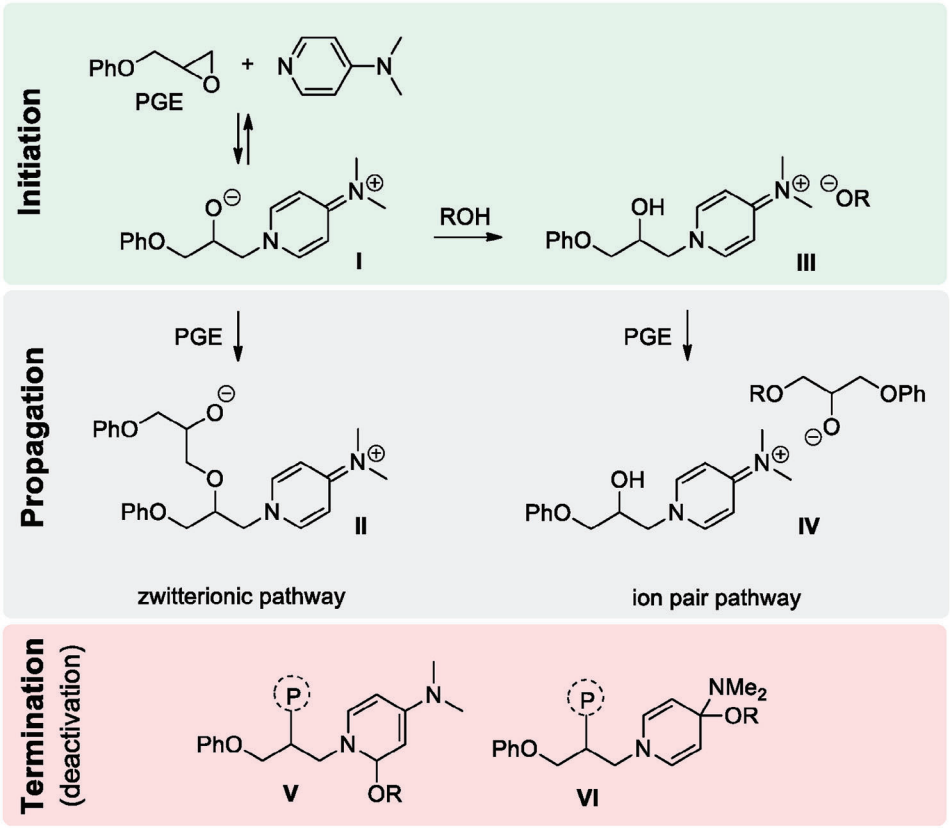

Scheme 4. Initiation, propagation and termination reactions during the polymerization of phenyl glycidyl ether (PGE) with DMAP (P in the dotted circle represents the polymer chain).

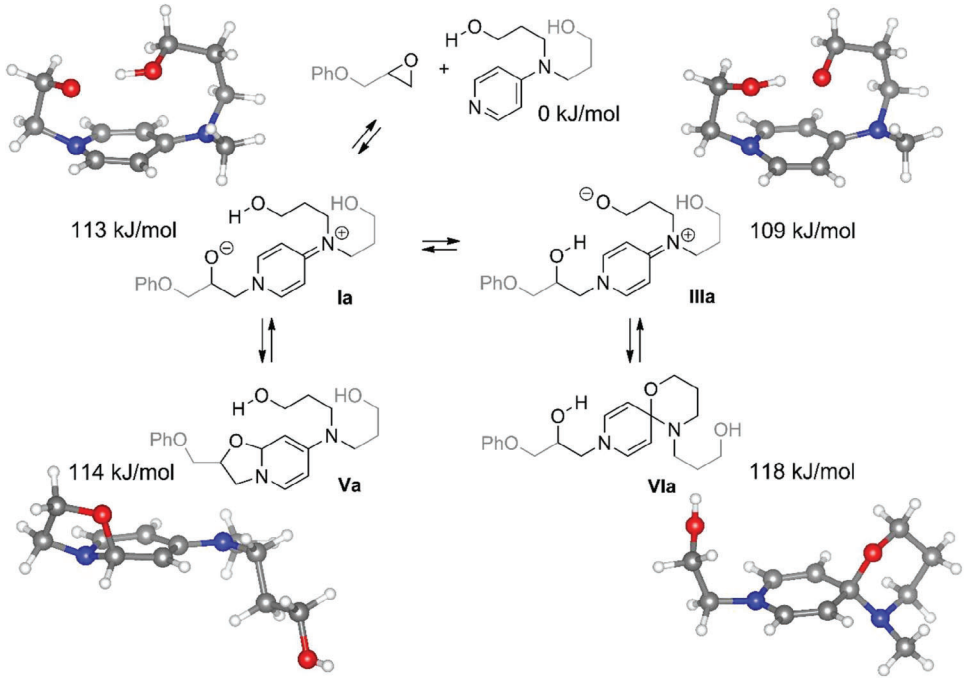

Figure 5. Chemical structures of the postulated zwitterions Ia and IIIb and potential reaction pathways leading to neutral molecules Va and VIa. Grey parts of the structures illustrate the parts of the molecules that were omitted in the calculations to reduce computational cost. Relative energies of Ia–VIa with respect to the respective starting materials and lowest-energy conformers of the calculated model structures are shown. All calculations were performed using B3LYP.

starting point for the irreversible termination of DMAP derivative-promoted epoxy-homopolymerizations and epoxy-alcohol reactions. This pathway might be particularly important for the deactivation of 3a and 3b in the epoxy-homopolymerization at temperatures above 100 °C.

3. Conclusion

The aza-Michael reaction enables a simple and modular alkylation reaction of aminopyridine derivatives, introducing functional groups in the periphery of the electron-rich pyridine core. The presence of hydroxyl groups in the initiator is of particular interest because it provides a faster homopolymerization of phenyl glycidyl ether at 100 °C than the parent 4-dimethylaminopyridine. However, epoxy homopolymerization and the epoxy alcohol reaction initiated with all electron-rich pyridine derivatives under investigation are irreversibly terminated at temperatures above 100 °C. The termination reaction is particularly rapid at higher alcohol concentrations.

4. Experimental Section

Chemicals: Chemicals were purchased from Sigma-Aldrich, Fisher Scientific, Merck, or Alfa Aesar. All reagents were used without further purification unless otherwise noted. 1,2,3,4-Tetrahydropyrido[3,4-b]pyrazine was prepared according to literature.[24]

Analytical Techniques: NMR spectra were recorded on a Bruker Avance III 300 MHz FT NMR spectrometer (300.36 MHz [^{1}H], 75.53 MHz [^{13}C]). Chemical shifts δ [ppm] were referenced to residual protonated solvent signals as internal standard $CDCl_3$: δ = 7.26 ppm (^{1}H), 77.16 ppm (^{13}C). Elemental analyses were conducted on an Elementar Vario Micro Cube with a CHN detector. Analytical thin layer chromatography (TLC) was performed on Merck silica gel 60-F_{254}, and spots were visualized by UV light or by treatment with cerium ammonium molybdate solution or potassium permanganate. Column chromatography was performed using silica gel 60 Å from Acros Organics. Size exclusion chromatograph was carried out with a Knauer system (with the AZURA P 6.1L isocratic pump and the AZURA RID 2.1L refractometer as the key components) operated with the ClarityChrom software. Columns were purchased from Applichrom GmbH (StyDiViBe-P-100A and StyDiViBe-P-500A were used in series), THF was used as the solvent, and calibration was done against poly(styrene standards). Thermogravimetric analysis (TGA) was performed with a Netzsch simultaneous thermal analyzer STA 449C (crucibles: Aluminum from Netzsch). The heating rate was 10 °C min^{-1} until a final temperature of 550 °C was reached. A helium flow of 20 cm^3·min^{-1} was used in combination with a protective flow of helium of 10 cm^3·min^{-1}. DSC measurements were performed on a PerkinElmer DSC 8500 instrument using aluminum sealed pans. In the case of dynamic measurements, the heat of polymerization (ΔH_0) was determined from the integration of the peak area of the corresponding thermogram according to Equation (1).

$$\Delta H_0\left[\frac{kJ}{mol}\right] = \frac{peakarea\left[\frac{mW}{mg} * K\right]}{heatrate\left[\frac{K}{s}\right]} * \frac{m_{epoxy} + m_{alcohol} + m_{cat}\,[mg]}{Nrofepoxides\,[mmol]} / 1000 \quad (1)$$

In the case of isothermal measurements, ΔH^0 was determined from the integration of the peak area of the corresponding thermogram according to Equation (2).

$$\Delta H_0\left[\frac{kJ}{mol}\right] = peakarea\left[\frac{mW}{mg} * \min\right] * \frac{m_{epoxy} + m_{cat}\,[mg]}{Nrofepoxides\,[mmol]} / \frac{60}{1000} \quad (2)$$

Computational Details: Conformational searches of all structures were performed with the COSMO-conf program at the PBE-D3/def2-SVPD level.[39,40] The lowest energy structures were then reoptimized using PBE-D3/def2-SVPD as implemented in ORCA (version 5.0.2).[41] Confirmation of the minima, calculation of zero-point vibrational energies, and thermal properties (at 25 °C) were performed by calculation of analytical normal modes using the rigid-rotor harmonic oscillator (RRHO) approximation. The structures were used as input geometries for further optimization using the double-hybrid functional B3LYP-D3, the def2-TZVPPD basis set, and D3 dispersion correction.[42,43] The best estimate for the calculation of Gibbs free energies (ΔG) resulted in using B3LYP-D3/def2-TZVPPD + ZPE,temp (PBE-D3/def2-SVPD). Gibbs free energies were obtained by calculating the energy differences between products and starting materials.

Synthesis of 3,3′-(4-Pyridinylimino)bis[propanenitrile] (1a): A mixture of 4-aminopyridine (1.88 g, 0.020 mol) and acrylonitrile (13 cm^3, excess) was stirred for 24 h at 80 °C. The formed participates were filtered off, washed with acetone, and dried in vacuum giving 2.73 g (68%) of a white solid.

R_f (CH_2Cl_2/MeOH = 20/1) = 0.21; ^{1}H-NMR (300 MHz, DMSO-d_6, 25 °C): δ = 8.16 (d, 2H, $^3J_{HH}$ = 6.5 Hz, py^{2,6}), 6.79 (d, 2H, $^3J_{HH}$ = 6.5 Hz, py^{3,5}), 3.74 (t, 4H, NCH_2CH_2), and 2.76 (t, 4H, CH_2CH_2CN) ppm. ^{13}C{^{1}H}-NMR (75 MHz, DMSO-d_6, 25 °C): δ = 151.1 (1C, py^4), 149.9 (2C, py^{2,6}), 119.1 (1C, N≡*C*-), 107.1 (2C, py^{3,5}), 44.6 (2C, NCH_2CH_2), and 15.1 (2C, CH_2CH_2CN) ppm. Spectra in accordance with refs. [25, 26].

3,3′-(2,3-Dihydropyrido[3,4-b]pyrazine-1,4-diyl)bis[propanenitrile] (1b): A mixture of 1,2,3,4-tetrahydropyrido[3,4-b]pyrazine (200 mg, 1.48 mmol) and acrylonitrile (1 cm^3, excess) was stirred for 24 h at 80 °C. Volatiles were removed in vacuum and the resulting oily brown residue was then purified by column chromatography (CH_2Cl_2/MeOH/TEA = 1500/100/1) on silica to afford upon drying in vacuum 218 mg (61%) of a yellow solid.

R_f = (CH_2Cl_2/MeOH/TEA = 1000/100/1) = 0.30; ^{1}H-NMR (300 MHz, $CDCl_3$, 25°C): δ = 7.87 (d, 1H, $^3J_{HH}$ = 6 Hz, py^7), 7.67 (s, 1H, pyr^5), 6.31 (d, ^{1}H, $^3J_{HH}$ = 6 Hz, pyr^8), 3.65 (m, 4H, NCH_2CH_2), 3.60, 3.45 (m, 4H, pyr^{2,3}), and 2.65 (m, 4H, CH_2CH_2CN) ppm. ^{13}C{^{1}H}-NMR (75 MHz, $CDCl_3$, 25 °C): δ = 141.6, 139.7, 131.6, 129.4 (4 C, pyr^{4a,5,7,8a}), 118.3, 117.9 (2C, CH_2CH_2CN), 104.5 (1C, pyr^8), 48.0, 47.1, 46.8 (4C, pyr^{2,3}, CH_2CH_2CN), and 15.1 (2C, CH_2CH_2CN) ppm. Anal. calcd. for $C_{13}H_{15}N_5$: C 65.98, H 6.04, N 27.98; found: C 66.14, H 5.87, N 28.12.

Synthesis of N-(3-Ethoxy-3-oxopropyl)-N-4-pyridinyl-β-alanine ethyl ester (2a): A mixture of 4-aminopyridine (1.88 g, 0.020 mol) and ethyl acrylate (11 cm^3, excess) was stirred at 80 °C for 24 h. Volatiles were removed in vacuum and the brown oily crude material was purified with column chromatography (CH_2Cl_2/MeOH/TEA = 90/10/1) on silica to afford a light brown solid (2.53 g, 43%).

R_f (CH_2Cl_2/MeOH/TEA = 90/10/1) = 0.45; ^{1}H-NMR (300 MHz, $CDCl_3$, 25 °C): δ = 8.24 (d, 2H, $^3J_{HH}$ = 5 Hz, py^{2,6}), 6.51 (d, 2H, $^3J_{HH}$ = 5 Hz, py^{3,5}), 4.15 (q, 4H, $^3J_{HH}$ = 7 Hz, OCH_2CH$_3$), 3.69 (t, 4H, $^3J_{HH}$ = 7 Hz, CH_2CH_2N), 2.59 (t, 4H, $^3J_{HH}$ = 7 Hz, CH_2CH_2N), and 1.25 (t, 6H, $^3J_{HH}$ = 7 Hz, OCH_2CH_3) ppm. ^{13}C{^{1}H}-NMR (75 MHz, $CDCl_3$, 25 °C): δ = 171.6 (2C, *C*OO), 151.8 (1C, py^4), 150.3 (2C, py^{2,6}), 106.9 (2C, py^{3,5}), 61.0 (2C, OCH_2CH_3), 45.9 (2C, CH_2CH_2N), 32.3 (2C, CH_2CH_2N), and 14.3 (2C, OCH_2CH_3) ppm. Spectra in accordance with ref. [28].

Synthesis of Diethyl 2-(((3-ethoxy-3-oxopropyl)(pyridin-4-yl)amino)methyl)pentanedioate (2a′): 2a′ was isolated from the reaction mixture obtained during the synthesis of 2a by column chromatography and giving 180 mg (2.3%) of a slightly yellow oil upon drying in vaccum.

R_f (CH_2Cl_2/MeOH/TEA = 90/10/1) = 0.50; ^{1}H-NMR (300 MHz, $CDCl_3$, 25 °C): δ = 8.23 (d, 2H, $^3J_{HH}$ = 5 Hz, py^{2,6}), 6.50 (d, 2H, $^3J_{HH}$ = 5 Hz, py^{3,5}), 4.19–3.99 (m, 6H, OCH_2CH$_3$), 3.75–3.60 (m, 3H, CH_2CH_2N, CHCH_2N), 3.42 (m, 1H, CHCH_2N), 2.83 (m, 1H, CH_2CHCH$_2$), 2.55 (t, 2H, CH_2CH_2N), 2.33 (m, 2H, CHCH$_2$CH_2COO), 1.89 (m, 2H, CHCH_2CH$_2$COO), and 1.31–1.11 (m, 9H, OCH_2CH_3) ppm. ^{13}C{^{1}H}-NMR (75 MHz, $CDCl_3$, 25 °C): δ = 173.4, 171.9, 170.9 (3C, *C*OO), 151.4 (1C, py^4), 149.7 (2C, py^{2,6}), 106.6 (2C, py^{3,5}), 60.4, 60.2, 60.0 (3C, OCH_2CH_3), 51.8 (1C, CHCH$_2$N), 45.5 (1C, CH_2CH_2N), 42.7 (1C, CHCH$_2$N), 31.18, 31.13 (2C, CH_2CH_2), 24.7 (1C, CHCH$_2$CH$_2$COO), and 13.71, 13.68, 13.63 (3C, OCH_2CH_3) ppm. Anal. calcd. for $C_{20}H_{30}N_2O_6$: C 60.90, H 7.67, N, 7.10; found: C 60.64, H, 7.39, N, 6.99.

Diethyl 3,3′-(2,3-dihydropyrido[3,4-b]pyrazine-1,4-diyl)dipropionate (2b): 2b was prepared analogously to 1b using 1,2,3,4-tetrahydropyrido[3,4-b]pyrazine (0.80 g, 5.9 mmol) and ethyl acrylate (3.5 cm^3, excess) as the starting materials. Purification was accomplished by column chromatography (CH_2Cl_2/MeOH/TEA = 2500/100/1) on silica to afford a light brown solid (0.79 g, 40%).

R_f (CH_2Cl_2/MeOH/TEA = 1000/10/1) = 0.40; ^{1}H-NMR (300 MHz, $CDCl_3$, 25 °C): δ = 7.80 (d, 1H, $^3J_{HH}$ = 6 Hz, pyr^7), 7.67 (s, 1H, pyr^5), 6.36 (d, 1H, $^3J_{HH}$ = 6 Hz, pyr^8), 4.14 (q, 4H, $^3J_{HH}$ = 7 Hz, OCH_2CH_3), 3.59, (m, 4H, pyr^{2,3}), 3.47, 3.29 (m, 4H, NCH_2CH_2), 2.59 (m, 4H, NCH_2CH_2), and 1.24 (t, 6H, $^3J_{HH}$ = 7 Hz, OCH_2CH_3) ppm. ^{13}C{^{1}H}-NMR (75 MHz, $CDCl_3$, 25 °C): δ = 171.9 (2C, *C*OO), 141.8, 139.9, 131.5, 129.3 (4C, pyr^{4a,5,7,8a}), 104.7 (1C, pyr^8), 61.2 (2C, OCH_2CH_3), 48.2, 47.4, 46.3, 45.9 (4C, pyr^{2,3}, CH_2CH_2COO), 32.3, 32.1 (2C, CH_2CH_2COO), and 14.3 (2C, OCH_2CH_3) ppm. Anal. calcd. for $C_{17}H_{25}N_3O_4$: C 60.88, H 7.51, N 12.53; found: C 61.06, H 7.33, N, 12.51.

3,3′-(Pyridin-4-ylazanediyl)bis(propan-1-ol) (3a): To a suspension of lithium aluminum hydride (245 mg, 6.5 mmol) in THF (12 cm^3) at 0 °C, a solution of 2a (1.14 g, 3.87 mmol) in THF (5 cm^3) was added dropwise over 10 min. The reaction mixture was vigorously stirred for 4 h at room temperature. Water was added dropwise to the stirred reaction mixture and the formed precipitate was filtered off and washed three times with THF (5 cm^3 each). The THF solution was dried over Na_2SO_4 and after evaporation of volatiles, a brown oily residue was obtained. The crude product was purified by recrystallization from acetonitrile (≈10 cm^3) releasing colorless crystals (0.49 g, 60%).

R_f (CH_2Cl_2/MeOH/TEA = 100/10/1) = 0.90; ^{1}H-NMR (300 MHz, $CDCl_3$, 25 °C): δ = 8.13 (d, 2H, $^3J_{HH}$ = 6 Hz, py^{2,6}), 6.53 (d, 2H, $^3J_{HH}$ = 6 Hz, py^{3,5}), 3.72 (q, 4H, $^3J_{HH}$ = 7 Hz, $NCH_2CH_2CH_2O$), 3.48 (t, 4H, $^3J_{HH}$ = 7 Hz, $NCH_2CH_2CH_2O$), and 1.85 (m, 4H, $NCH_2CH_2CH_2O$) ppm. ^{13}C{^{1}H}-NMR (75 MHz, $CDCl_3$, 25 °C): δ = 152.6 (1C, py^4), 149.7 (2C, py^{2,6}), 106.6 (2C, py^{3,5}), 59.9 (2C, $NCH_2CH_2CH_2O$), 46.7 (2C, $NCH_2CH_2CH_2O$), and 29.8 (2C, $NCH_2CH_2CH_2O$) ppm. Anal. calcd. for $C_{11}H_{18}N_2O_2$: C 62.83, H 8.63, N 13.32; found C 62.88, H 8.64, N 13.44.

Synthesis of 3,3′-(2,3-Dihydropyrido[3,4-b]pyrazine-1,4-diyl)bis(propan-1-ol) (3b): 3b was prepared analogously to 3a using lithium aluminum hydride (189 mg, 5 mmol) and 2b (600 mg, 1.79 mmol) as the starting materials resulting in a white solid (225 mg, 50%).

R_f (CH_2Cl_2/MeOH/TEA = 1000/10/1) = 0.10; ^{1}H-NMR (300 MHz, $CDCl_3$, 25 °C): δ = 7.70 (d, 1H, $^3J_{HH}$ = 6 Hz, pyr^7), 7.64 (s, 1H, pyr^5), 6.60 (d, 1H, $^3J_{HH}$ = 6 Hz, pyr^8), 3.65 (m, 4H, $^3J_{HH}$ = 6 Hz, $NCH_2CH_2CH_2O$), 3.47, 3.40, 3.25, 3.18 (m, 8H, pyr^{2,3}, $NCH_2CH_2CH_2O$), and 1.82 (4H, m, $NCH_2CH_2CH_2O$) ppm. ^{13}C{^{1}H}-NMR (75 MHz, $CDCl_3$, 25 °C): δ = 141.4, 140.7, 131.8, 130.9 (4C, pyr^{4a,5,7,8a}), 104.2 (1C, pyr^8), 61.0, 60.0 (2C, $NCH_2CH_2CH_2O$), 48.7, 47.5, 47.2, 46.1 (4C, N pyr^{2,3}, $CH_2CH_2CH_2O$), and 28.9, 28.6 (2C, $CH_2CH_2CH_2O$) ppm. Anal. calcd. for $C_{13}H_{21}N_3O_2$: C 62.13, H 8.42, N 16.72; found: C 62.23, H, 8.63, N, 16.89.

Supporting Information

Supporting Information is available from the Wiley Online Library or from the author.

Acknowledgements

Financial support by the Austrian Federal Ministry for Digital and Economic Affairs, the National Foundation for Research, Technology and Development, and the Christian Doppler Research Association (Christian Doppler Laboratory for Organocatalysis in Polymerization) is gratefully acknowledged. The authors thank A. Daniel Boese (University of Graz) for providing access to HPC resources.

Conflict of Interest

The authors declare no conflict of interest.

Data Availability Statement

The data that support the findings of this study are available from the corresponding author upon reasonable request.

Keywords

4-dimethylaminopyridine, aza-Michael reaction, epoxy-homopolymerization

Received: August 16, 2023
Revised: November 7, 2023
Published online: November 22, 2023

[1] G. Höfle, W. Steglich, H. Vorbrüggen, *Angew. Chem., Int. Ed.* **1978**, *17*, 569.
[2] D. J. Berry, C. V. Digiovanna, S. S. Metrick, R. Murugan, *ARKIVOC* **2001**, https://doi.org/10.3998/ark.5550190.0002.114
[3] F. Nederberg, E. F. Connor, M. Möller, T. Glauser, J. L. Hedrick, *Angew. Chem., Int. Ed.* **2001**, *40*, 2712.
[4] J. Helberg, T. Ampßler, H. Zipse, *J. Org. Chem.* **2020**, *85*, 5390.
[5] D. Edinger, H. Weber, E. Zagar, D. Pahovnik, C. Slugovc, *ACS Appl. Polym. Mater.* **2021**, *3*, 2018.
[6] K. Ratzenböck, S. M. Fischer, C. Slugovc, *Monatsh. Chem.* **2023**, *54*, 443.
[7] S. Strasser, C. Wappl, C. Slugovc, *Polym. Chem.* **2017**, *8*, 1797.
[8] K. Ratzenböck, M. M. Ud Din, S. M. Fischer, E. Zagar, D. Pahovnik, A. D. Boese, D. Rettenwander, C. Slugovc, *Chem. Sci.* **2022**, *13*, 6920.
[9] K. Ratzenböck, D. Pahovnik, C. Slugovc, *Polym. Chem.* **2020**, *11*, 7476.
[10] I. E. Dell'erba, R. J. J. Williams, *Polym. Eng. Sci.* **2006**, *46*, 351.
[11] X. Fernández-Francos, W. D. Cook, À. Serra, X. Ramis, G. G. Liang, J. M. Salla, *Polymer* **2010**, *51*, 26.
[12] C. H. Chen, Z. C. Gu, Y. L. Tsai, R. J. Jeng, C. H. Lin, *Polymer* **2018**, *140*, 225.
[13] B. Chen, Q. Zhang, M. Lu, H. Meng, Z. Qu, C. Xu, E. Jiao, *J. Appl. Polym. Sci.* **2021**, *138*, 50523.
[14] S. W. Shao, C. H. Chen, J. R. Chan, T. Y. Juang, M. M. Abu-Omar, C. H. Lin, *Green Chem.* **2020**, *22*, 4683.
[15] C.-M. Lin, C.-H. Chen, C.-H. Lin, W. C. Su, T.-Y. Juang, *ACS Omega* **2018**, *3*, 4295.
[16] W. Natongchai, J. A. Luque-Urrutia, C. Phungpanya, M. Solà, V. D'elia, A. Poater, H. Zipse, *Org. Chem. Front.* **2021**, *8*, 613.
[17] W. Natongchai, S. Posada-Pérez, C. Phungpanya, J. A. Luque-Urrutia, M. Solà, V. D'elia, A. Poater, *J. Org. Chem.* **2022**, *87*, 2873.
[18] M. Murayama, F. Sanda, T. Endo, *Macromolecules* **1998**, *31*, 919.
[19] K. E. Price, B. P. Mason, A. R. Bogdan, S. J. Broadwater, J. L. Steinbacher, D. T. McQuade, *J. Am. Chem. Soc.* **2006**, *128*, 10376.
[20] V. D'elia, Y. Liu, H. Zipse, *Eur. J. Org. Chem.* **2011**, *2011*, 1527.
[21] A. Y. Rulev, *Eur. J. Org. Chem.* **2023**, *26*, 202300451.
[22] S. Shimizu, N. Watanabe, T. Kataoka, T. Shoji, N. Abe, S. Morishita, H. Ichimura, *Pyridine and Pyridine Derivatives in Ullmann's Encyclopedia of Industrial Chemistry*, Wiley-VCH, Weinheim, Germany **2007**. https://doi.org/10.1002/14356007.a22_399
[23] F. Garavaglia, A. Barozza, J. Roletto, P. Paissoni, *Eur. Patent 2394994 A1* **2011**.
[24] I. Held, S. Xu, H. Zipse, *Synthesis* **2007**, *10*, 1185.
[25] J. Ni, Y.-Z. Li, W.-B. Qi, Y.-J. Liu, H.-L. Chen, Z.-L. Wang, *Acta Crystallogr., Sect. C: Cryst. Struct. Commun.* **2003**, *C59*, o470.
[26] P. Buckus, A. Buckiene, *Russ. J. Gen. Chem.* **1963**, *33*, 56613
[27] J. Huang, J. Sun, A. Cao, Z. Liu, S. Shao, *Huaxue Shijie* **1994**, *35*, 9635
[28] H. Nishida, *World Patent 2003095446 A1* **2003**.

[29] E. J. Delaney, L. E. Wood, I. M. Klotz, *J. Am. Chem. Soc.* **1982**, *104*, 799.
[30] I. M. Klotz, S. E. Massil, L. E. Wood, *J. Polym. Sci., Polym. Chem. Ed.* **1985**, *23*, 575.
[31] S. M. Fischer, V. Schallert, J. M. Uher, C. Slugovc, *Polym. Chem.* **2023**, *14*, 1081.
[32] K. Kodolitsch, F. Gobec, C. Slugovc, *Eur. J. Org. Chem.* **2020**, *19*, 2973.
[33] A. Fantoni, T. Koch, S. Baudis, R. Liska, *ACS Appl Polym. Mater.* **2023**, *5*, 731.
[34] B. A. Rozenberg, *Adv. Polym. Sci.* **1986**, *75*, 113.
[35] X. Fernàndez-Francos, *Eur. Polym. J.* **2014**, *55*, 35.
[36] X. Fernández-Francos, A.-O. Konuray, A. Belmonte, S. De La Flor, À. Serra, X. Ramis, *Polym. Chem.* **2016**, *7*, 2280.
[37] N. Kratena, B. Marinic, T. J. Donohoe, *Chem. Sci.* **2022**, *13*, 14213.
[38] Y.-P. Lam, X. Wang, F. Tan, W.-H. Ng, Y.-L. S. Tse, Y.-Y. Yeung, *ACS Catal.* **2019**, *9*, 8083.
[39] J. P. Perdew, K. Burke, M. Ernzerhof, *Phys. Rev. Lett.* **1996**, *77*, 3865.
[40] S. Grimme, J. Antony, S. Ehrlich, H. Krieg, *J. Chem. Phys.* **2010**, *132*, 154104.
[41] F. Neese, *Wiley Interdiscip. Rev.: Comput. Mol. Sci.* **2018**, *8*, 1327.
[42] A. D. Becke, *Phys. Rev. A* **1988**, *38*, 3098.
[43] S. Grimme, *J. Chem. Phys.* **2006**, *124*, 034108.